Discovery and Validation of Pyridoxic Acid and Homovanillic Acid as Novel Endogenous Plasma Biomarkers of Organic Anion Transporter (OAT) 1 and OAT3 in Cynomolgus Monkeys

Hong Shen, David M. Nelson, Regina V. Oliveira, Yueping Zhang, Colleen A. Mcnaney,

Xiaomei Gu, Weiqi Chen, Ching Su, Michael D. Reily, Petia A. Shipkova,

Jinping Gan, Yurong Lai, Punit Marathe, and W. Griffith Humphreys

Departments of Metabolism and Pharmacokinetics (H.S., Y.Z., X.G., W.C., J.G., Y.L., P.M., W.G.H.), Discovery Toxicology (D.N., C.A.M., M.D.R.), Bioanalytical Research (R.O., P.A.S.), and Discovery Pharmaceutics (C.S.), Pharmaceutical Candidate Optimization, Bristol-Myers Squibb Research and Development, Princeton, New Jersey 08543, United States

1

Running title: Identification of functional plasma markers of OAT1 and OAT3 in vivo

Address correspondence to:

Dr. Hong Shen

Department of Metabolism and Pharmacokinetics (MAP)

Pharmaceutical Candidate Optimization (PCO)

Bristol-Myers Squibb Company (BMS)

Route 206 & Province Line Road, Princeton, NJ 08543-4000

Telephone: (609) 252-4509

Facsimile: (609) 252-6802

E-mail: hong.shen1@bms.com

Number of text pages: 29

Number of tables: 3

Number of figures: 6

Number of references: 39

Number of words:

Abstract: 249

Introduction: 794

Discussion: 1832

Abbreviations: A_e, amount of unchanged drug recovered in the urine; AUC, area under the plasma concentration-time curve; CCK-8, cholecystokinin octapeptide; CE, collision energy; CL_{NR},

nonrenal plasma clearance; CL_R, renal clearance; CL_{TOT}, total plasma clearance; CsA, cyclosporin

A; DCA, dicarboxylic acid; DMEM, DDI, drug-drug interaction; Dulbecco's modified Eagle's

growth medium; DP, declustering potential; E3S, estrone-3-sulfate; E17βG, estradiol-17β-D-

glucuronide; f_{NR}, the fraction excreted by nonrenal routes; f_R, fraction excreted in the urine; FSM,

furosemide; GA, glucuronic acid; GFR, glomerular filtration rate; HBSS, Hanks' balanced salt

solution; HEK, human embryonic kidney; HDA, hexadecanedioic acid; HVA, homovanillic acid;

IC_{50}, concentration required to inhibit transport by 50%; IMC, indomethacin; K_m, Michaelis-

Menten constant that corresponds to the substrate concentration at which the uptake rate is half of

V_{max}; LC-MS/MS, liquid chromatography–tandem mass spectrometry; MATE, multidrug and

toxin extrusion protein; MFM, metformin; NTCP, sodium taurocholate cotransporting

polypeptide; OAT, organic anion transporter; OATP, organic anion transporting polypeptide;

OCT, organic cation transporter; PAH, *para*-aminohippuric acid; PBS, phosphate-buffered saline;

PCV, penciclovir; PDA, pyridoxic acid; PROB, probenecid; PYR, pyrimethanmine; RPTC, renal

proximal tubule cell; SRM, selective reaction monitoring; TCA, taurocholic acid; TDA,

tetradecanedioic acid, V_{max}, maximum transport rate.

ABSTRACT:

Perturbation of OAT1- and OAT3-mediated transport can alter the exposure, efficacy, and safety of drugs. Although these have been reports of the endogenous biomarkers for OAT1/3, none of these have all of the characteristics required for a clinical useful biomarker. Cynomolgus monkeys were treated with intravenous probenecid (PROB) at a dose of 40 mg/kg in this study. As expected, PROB increased the *AUC* of co-administered furosemide (FSM), a known substrate of OAT1 and OAT3, by 4.1-fold, consistent with the values reported in humans (3.1- to 3.7-fold). Of 233 plasma metabolites analyzed using a LC-MS/MS-based metabolomics method, 29 metabolites, including pyridoxic acid (PDA) and homovanillic acid (HVA), were significantly increased at either 1 or 3 h in plasma from the monkeys pretreated with PROB compared with the treated animals. Plasma of animals was then subjected to targeted LC-MS/MS analysis which confirmed that the PDA and HVA *AUC*s increased by approximately 2- to 3-fold by PROB pretreatments. PROB also increased plasma concentrations of hexadecanedioic acid (HDA) and tetradecanedioic acid (TDA) although the increases were not statistically significant. Moreover, transporter profiling assessed using stable cell lines constitutively expressing transporters, demonstrated that PDA and HVA are substrates for human OAT1, OAT3, OAT2 (HVA) and OAT4 (PDA), but not OCT2, MATE1, MATE2K, OATP1B1, OATP1B3, and NTCP. Collectively, these findings suggest that PDA and HVA might serve as blood-based endogenous probes of cynomolgus monkey OAT1 and OAT3, and investigation of PDA and HVA as circulating endogenous biomarkers of human OAT1 and OAT3 function is warranted.

4

INTRODUCTION

OAT1 (*SLC*22A6) and OAT3 (*SLC*22A8) function as influx-transporters that are mainly expressed on the basolateral membrane of renal proximal tubular cells (RPTCs) and mediate cellular uptake of substrates from blood into the cells (Motohashi et al., 2002). OAT1 and OAT3 can serve as the loci of drug-drug interactions (DDIs), and such DDIs can lead to undesired changes in systemic and local exposures of victim drugs and toxins (Morrissey et al., 2013; Nigam et al., 2015). For example, furosemide (FSM) is taken up from the blood in RPTCs via OAT1 and OAT3 (Hasannejad et al., 2004), and probenecid (PROB), an inhibitor of OAT1 and OAT3, causes significant alterations in the pharmacokinetic parameters of FSM in humans through increased area under the plasma drug concentration-time curve (AUC), decreased total and renal clearance (CL_{TOT} and CL_R), and decreased fraction excreted in the urine (f_R) (Chennavasin et al., 1979; Smith et al., 1980; Vree et al., 1995). Moreover, a few uremic toxins recently have been demonstrated to be inhibitors of OAT1 and OAT3, and have the potential to inhibit renal secretion clearance of drug substrates of OAT1 and OAT3 in patients with chronic kidney disease (Hsueh et al., 2016). On the other hand, concomitant use of PROB is recommended by the United States Food and Drug Administration (FDA) for reducing the pronounced nephrotoxicity of cidofovir by inhibiting OAT1 and OAT3 to reduce the exposure of cidofovir in RPTCs to an extent that results in an acceptable benefit-risk balance (http://www.accessdata.fda.gov/drugsatfda_docs/label/1999/020638s003lbl.pdf).

Animal models have often been often used to assess pre-clinical drug-OAT interactions. For example, the clinical famotidine-PROB interaction was reproduced in cynomolgus monkeys recently as PROB caused an approximate 90% reduction in the tubular secretion clearance of famotidine in monkeys (4.58 ± 1.25 versus 0.38 ± 0.36 mL/min/kg) (Tahara et al., 2006). Similarly,

PROB significantly decreased the renal tubular secretion clearance of famotidine from 2.80 ± 0.36 to 0.37 ± 0.07 mL/min/kg in humans. Furthermore, the protective effect of PROB treatment on the nephrotoxicity of cidofovir in humans was able to be recapitulated in monkeys (Lacy et al., 1998). These results suggest that monkey is the more suitable animal model to predict the clinical DDIs involving OAT1 and OAT3.

Recently endogenous biomarkers have been envisioned as a simple, fast, and cost-effective tool to monitor transporter activity in a preclinical and clinical setting to facilitate development of a drug candidate (Bergagnini-Kolev et al., 2017; Ito et al., 2012; Lai et al., 2016; Muller et al., 2015; Yee et al., 2016). Therefore, the identification of a sensitive endogenous biomarker for OAT1 and OAT3 would be of great value. In this regard, Imamura et al. reported that 6β-hydroxycortisol could be an endogenous probe for OAT3 inhibition evaluation as PROB significantly changed the AUC and CL_R of 6β-hydroxycortisol in healthy subjects (Imamura et al., 2014). However, 6β-hydroxycortisol is formed from cortisol by hepatic CYP3A4, and many drugs are known to affect this drug-metabolizing enzyme can also change exposure of 6β-hydroxycortisol (Peng et al., 2011). Very recently Tsuruya et al. reported that taurine and glycochenodeoxycholate sulfate (GCDCA-S) were endogenous biomarkers of OAT1 and OAT3, respectively (Tsuruya et al., 2016). However, the plasma levels of taurine and GCDCA-S were not changed significantly by PROB treatment compared to control even though the renal secretion and CL_R were significantly decreased (Tsuruya et al., 2016). Reduced activities of blood-facing OAT1 and OAT3 by PROB are supposed to increase plasma concentration of a sensitive and selective endogenous probe, mimicking systemic alterations of probe drugs such as FSM. To our knowledge, all published "endogenous biomarkers" of OAT1 and OAT3 could not recapitulate plasma drug concentration time profiles in the presence of OAT inhibitors. Several features

including specificity, sensitivity, predictability, reproducibility, acute response and accessibility have been considered in the identification and validation of ideal endogenous biomarkers for drug transporters (Chu et al., 2017; Mariappan et al., 2017; Rodrigues et al., 2017). Given the aforementioned reasons, there is a need for novel plasma biomarkers of renal organic anion transporters.

In the present studies we provide direct experimental evidence that several organic anionic compounds, including pyridoxic acid (PDA), homovanilic acid (HVA), hexadecanedioic acid (HDA) and tetradecanedioic acid (TDA) are potential endogenous biomarkers of OAT1 and OAT3 in cynomolgus monkeys. Specifically, an untargeted metabolomics analysis was applied to plasma samples to screen endogenous compounds that were associated with OAT1 and OAT3 inhibition in monkeys. Follow-up quantitative LC/MS analysis further characterized the time-plasma concentration profiles of selected endogenous compounds (i.e., PDA, HVA, HDA and TDA) after PROB administration in cynomolgus monkeys. Moreover, transporter profiling assessed using human embryonic kidney (HEK) 293 cells stably transfected with major human renal and hepatic drug transporters demonstrated that PDA and HVA are OAT1 and OAT3 substrates and thus potential novel plasma endogenous biomarkers of OAT1 and OAT3 inhibition.

MATERIALS AND METHODS

Materials. [³H]Penciclovir (PCV) (1.3 Ci/mmol) and [¹⁴C]metformin ([¹⁴C]MFM) (98 mCi/mmol) were purchased from Moravek Biochemicals, Inc. (Brea, CA). [³H]*para*-Aminohippuric acid (PAH) (4.5 Ci/mmol), [³H]estrone-3-sulfate ([³H]E3S; 44.0 Ci/mmol), [³H]estradiol-17β-D-glucuronide ([³H]E17βG) (34.3 Ci/mmol), and [³H] cholecystokinin octapeptide ([³H]CCK-8) (97.5 mCi/mmol) were purchased from PerkinElmer Life and Analytical Sciences (Waltham, MA). Nonradiolabeled furosemide (FSM), probenecid (PROB), taurocholic acid (TCA), and the corresponding stable isotope labeled internal standards were purchased from Toronto Research Chemicals Inc. (North York, Ontario). 4-Pyridoxic Acid (PDA, ≥98%) was purchased from Sigma Aldrich (St. Louis, MO), and Homovanilic acid (HVA, ≥98%) was purchased from Acros Organics. Hexadecanedioic acid-d28, tetradecanedioic acid-d24, and enalapril maleate-d5 (Enal-d5) were obtained from CDN Isotopes (Pointe-Claire, Quebec, Canada). Other nonradiolabeled compounds were purchased from either Sigma-Aldrich (St. Louis, MO) or Research Chemicals Inc. (North York, Ontario). and were of analytical grade. Cell culture media and reagents were purchased from Invitrogen (Carlsbad, CA) or Mediatech, Inc., A Corning Subsidiary (Manassas, VA).

Cynomolgus Monkeys Pharmacokinetic FSM-PROB Interaction Study Protocol. To identify and verify the endogenous biomarkers of OAT1 and OAT3, we conducted a series of experiments: cynomolgus monkey FSM-PROB interaction, metabolomics, targeted LC-/MS/MS, and transporter profiling experiments. The experimental workflow is shown in Figure 1.

A single-dose, three-period crossover intravenous (IV) pharmacokinetic DDI study was carried out at Bristol-Myers Squibb Company, and 3 male cynomolgus monkeys with body weights ranging from 5.3 to 6.0 kg during study periods were included in this study. The

experiment was performed in accordance with the National Institutes of Health guidelines and approved by Bristol-Myers Squibb Animal Care and Use Committee. The animals were housed in a temperature- and humidity-controlled room with a 12-h light/dark cycle.

In the first period, 40 mg/kg PROB dissolved in a sodium hydroxide solution (0.1 N) and titrated to neutral pH with hydrochloric acid was intravenously infused via a femoral vein catheter over 5 minutes (min) (5 mL/kg). Venous blood samples (2 mL) were collected before and 0.08, 0.17, 0.25, 0.5, 0.75, 1, 2, 3, 5, 7, and 24 hours (h) after administration in K2-EDTA-containing tubes.

In the second period, after a washout period of 7 days, 2 mg/kg FSM dissolved in saline was intravenously infused via a femoral vein over 5 min (5 mL/kg), and blood samples were collected before and 0.08, 0.17, 0.25, 0.5, 0.75, 1, 2, 3, 5, 7, and 24 h after administration. In the third period, 8 days after administrations of the previous dose of FSM, a FSM saline solution (2 mg/kg) was given by femoral vein infusion over 5 min to each monkey 30 min after PROB administration (40 mg/kg, IV infusion for 5 min). Blood was sampled before and 0.08, 0.17, 0.25, 0.5, 0.75, 1, 2, 3, 5, 7, and 24 h after start of the FSM infusion. Blood samples were spun for 5 min at 13,000 rpm within 1 h to obtain plasma. Urine samples were collected using metabolic cages for the following intervals in all 3 periods: 0 to 3 h, 3 to 7 h and 7 to 24 h after administration, and the volume of urine was recorded. The plasma and urine samples were stored at -80°C until liquid chromatography–tandem mass spectrometry (LC-MS/MS) and metabolomics analysis was conducted.

LC-MS/MS Analysis of Furosemide and Probenecid. The LC-MS/MS analysis was performed on a Sciex Triple Quad API-4000 system (AB Sciex, Framingham, MA) coupled with a Shimadzu Nexera LD-30AD ultra-performance liquid chromatography (UPLC) system

(Shimadzu, Columbian, MD). The chromatographic separation was performed on an Agilent Zorbax RRHD SB-C8 column (2.0 x 100 mm, 1.7 µm) from Agilent Technologies (Santa Clara, CA) using mobile phases of 0.1% formic acid in water and 0.1% formic acid in acetonitrile. The flow rate was 0.7 ml/min and total run time was 3.7 min. The LC column was maintained at 60 °C. The analytes were monitored using selected reaction monitoring (SRM) in negative ionization mode with the optimized nebulizing and desolvation gases. The source temperature was set at 400 ºC, and declustering potential (DP) and collision energy (CE) were optimized. Furosemide, furosemide-d5 and probenecid were detected at the SRM transitions of m/z 329.1 → 285.0, 334.1→291.0 and 283.9 → 239.9, respectively.

Before the analysis, urine samples were diluted 100 fold into blank plasma and treated as for plasma. The plasma and diluted urine samples were then extracted using protein precipitation. Specifically, the 100 µL plasma and diluted urine samples were mixed with 100 µL of acetonitrile containing 400 nM of furosemide-d5 (internal standard), followed by vortex mixing on a mixer for 5 min at room temperature. The mixed solutions were then filtered using MultiScreen hydrophilic flitration plate (Millipore, MA) by centrifugation at 4,000g for 10 min, and the filtered solution was then injected (5 µL) on to LC-MS/MS. The assay was qualified over the analytical range of 1 to 5,000 nM using a linear $1/x^2$ weighed regression.

Plasma Metabolomic Profiling. Frozen plasma samples were thawed and 50 µL aliquots were subjected to protein precipitation by the addition of 600 µL of methanol containing 0.1% formic acid and stable-labeled internal standards. The samples were mixed with a vortex mixer and subjected to centrifugation for 10 min at 2700 x g (4,000 rpm). An aliquot (50 µL) of the resulting supernatants were transferred to a 96-well plate for further hydrophilic interaction liquid

chromatography (HILIC) LC-MS analysis and an additional 100 μL were transferred to a separate 96-well plate for reverse phase (RP) LC-MS analysis. Both plates were dried to completeness under a nitrogen stream at room temperature. For RP LC-MS analysis, the dried samples were reconstituted by the addition of 20 μL of methanol, followed by vigorous shaking and the addition of 180 μL of water. The samples were mixed with a vortex mixer and subjected to centrifugation for 10 min at 4,000 rpm. The resulting supernatants were transferred to a 96-well plate, from which 10 μL were directly injected for analysis. For HILIC LC-MS analysis, the dried samples were reconstituted by the addition of 20 μL of water, followed by vigorous shaking and the addition of 180 μL of 50:50 MeOH:ACN. The samples were mixed with a vortex mixer and subjected to centrifugation for 10 min at 4000 rpm. The resulting supernatants were transferred to a 96-well plate, from which 10 μL were directly injected for analysis.

HILIC and RP LC- MS analyses were performed on a Nexera X2 LC-30AD (Shimadzu, Somerset, NJ) UHPLC system connected to a Exactive Plus (Thermo Fisher Scientific, Waltham, MA) mass spectrometer. The UHPLC column for HILIC analyses was an Acquity BEH-NH2, 2.1x150mm, 1.7 u (Waters Corporation, Milford, MA) with mobile phases A (95:5 water:ACN, 10 mM NH4OAc, 0.05% NH4OH) and B(ACN, 0.05% NH4OH) at a flow rate of 300 μL /min with starting conditions of 95%B to 37%B at 3.5 min, hold for 4 min and down to starting conditions at 7min, for a total run time of 11 min. The UHPLC column for RP analyses was an Acquity BEH C18, 2.1x150mm, 1.7 u (Waters Corporation, Milford, MA) with mobile phases A (water, 0.1% formic acid) and B (98:2ACN: water, 0.1% formic acid) at a flow rate of 600 μL /min with starting conditions of 100%A, to 80%A at 3 min, 40%A at 4min and 100%B by 7min and after a 2 min hold, down to starting conditions at 9 min, for a total run time of 11 min. Both

HILIC and RP LC-MS data was collected in positive and negative polarities (separate injections) at 35,000 resolution and expected mass accuracy of 5 ppm.

LCMS data analysis was performed using in-house developed software, Expedient Data Mining (EDM) as described previously (Hnatyshyn et al., 2013). Direct data input from raw files was performed using Thermo Fisher Scientific$^{®}$ MSFileReader software. The resulting list of components were matched with accurate mass and retention time values using an in-house database of endogenous metabolites stored within EDM. The annotated table of component integrals was exported to Microsoft$^{®}$ Excel for further statistical analysis using in-house Visual Basic scripts for Microsoft$^{®}$ Excel. For these analyses, mean intensities for each treatment group were compared to the relevant concurrent control. For each component, fold-change was calculated by dividing the treatment group value by the control group value and p-values were calculated as a pair-wise comparison for a two-tailed distribution, using Student's t-test (Excel statistics package, Microsoft$^{®}$).

Characterization of PDA and HVA Uptake in Stable Cell Lines Constitutively Expressing Major Renal Drug Transporters. Uptake studies were performed as described previously (Shen et al., 2016b). Uptake of PDA and HVA were first measured at a single concentration for 5-min incubation with OAT1-, OAT2-, OAT3-, OAT4-, OCT2-, MATE1-, MATE2K-, OATP1B1-, OATP1B3-, and NTCP-HEK cells, and then time- and concentration dependent uptake was measured. The initial concentration used for PDA was 1 μM because the physiological baseline level ranged from 0.67 to 2.5 μM in cynomolgus monkeys (Figure 3A). The concentration studied for HVA was 5 μM because of limited bioanalytical sensitivity of this compound in Mock-HEK cells. In addition, the transport Michaelis-Menten constant value (K_m)

value of 274 ± 100 μM has been reported in rat Oat2-mediated transport for HVA (Mori et al., 2003), which is significantly greater than the selected testing concentrations (274 ± 100 versus 5 μM). No corresponding data were available for PDA. Kinetic transport experiments were conducted under linear-uptake conditions or for shortest incubation duration with acceptable analytical sensitivity (Supplemental Figure 1).

Cells were grown to confluence in 24-well poly-D-lysine-coated plates 2 to 3 days after seeding at cell density of 500.000 cells per well (BD Biosciences, San Jose, CA). All experiments were conducted at 37°C using a working solution containing Hanks balanced salt solution (HBSS) supplemented with 10 mM HEPES (pH 7.4 for OAT1-, OAT2-, OAT3-, OAT4-, OCT2-, OATP1B1, OATP1B3-, and NTCP-HEK cells, and pH 8.4 for MATE1- and MATE2K-HEK cells, respectively), with a probe substrate, PDA, or HVA. The probe substrates used were [^{3}H]PAH (OAT1), [^{3}H]PCV (OAT2), [^{3}H]E3S (OAT3 and OAT4), [^{14}C]MFM (OCT2, MATE1, and MATE2K), [^{3}H]E17βG (OATP1B1), [^{3}H]CCK-8 (OATP1B3, and TCA (NTCP). Compounds were dissolved in dimethyl sulfoxide and diluted in Hanks balanced salt solution (HBSS) (maximum 0.2% dimethyl sulfoxide). Plating medium was removed, and cell monolayers were rinsed twice with prewarmed HBSS. Incubations were started by the addition of 200 μL of substrate prewarmed at 37°C. After incubation for desired time at 37°C, the cell monolayers were rinsed three times with 500 μL of ice-cold HBSS. The cells were then lysed with 300 μL buffer (0.1% Triton X-100 or methanol), and compound concentrations in the cell lysates were measured by either liquid scintillation counting (Tri-Carb 2910 TR Liquid Scintillation Analyzer, PerkinElmer Life and Analytical Sciences, Waltham, MA) or LC–MS/MS as described below.

LC-MS/MS Analysis of PDA and HVA. Stock PDA solution (390 μg/mL, 2.13 mM) was prepared by dissolving PDA in 0.5% NH4OH solution. Stock HVA (1.8 mg/mL, 9.5mM) solution

13

was prepared in water. Stock solutions were stored in darkness at -30°C and brought to room temperature before use. The highest calibration standard (5000 ng/mL) was prepared by diluting appropriate aliquots of PDA and HVA stock solutions to a final volume of 2 mL with 1% BSA in PBS (pH 7.4). Additional standard solutions were obtained by serial dilution from the 5000 ng/mL standard with 1% BSA in PBS (pH 7.4) to final concentrations of 2500, 1000, 500, 250, 100, 50, 25, 10 and 5 ng/mL. Quality control (QC) samples were also prepared with 1% BSA in PBS (pH 7.4) at three concentration levels: 7.5 ng/mL, 75 ng/mL and 750 ng/mL. The IS stock solution of Enal-d5 was prepared at 1 mg/mL in methanol. The IS working solution containing 1000 ng/mL of Enal-d5 was prepared by dilution of IS stock solution with methanol and stored at 4°C.

Calibration curves for PDA and HVA were fitted by 1/x weighted least squares quadratic. The calibration curves for PDA and HVA range from 5 to 5000 ng/mL. All coefficients of determination (R^2) of the calibration lines were ≥0.98. The mean accuracy (% of true value) of individual calibrators was ≥ 15%. The lower limit of quantitation (LLOQ), defined as the lowest concentration which could be determined with precision and accuracy of ± 20%, was 5ng/mL for PDA and HVA.

Samples stability was also determined for QCs samples (n = 5) that were extracted and stored in the instrument autosampler under refrigerated conditions (5°C). Samples were stable for 24 hrs. Average recovery for QCs samples (n = 5) prepared with 1% BSA in PBS (pH 7.4) was 101% and 102% for PDA and HVA, respectively.

Urine and plasma samples were diluted by a factor of 1:1, 1:2, 1:10 or 1:100 with 1% BSA in PBS (pH 7.4) to ensure levels within the range of the calibration curve. Aliquots (50 µL) of diluted animal samples (urine and plasma), calibrators standards or QCs were transferred to a 2

mL 96-well plate and mixed for 1 min at 2000 rpm. The samples were extracted by adding 200 µL

of Enal-d5 in methanol (1000 ng/mL) and vortex-mixed for 5 min at 2000 rpm, centrifuged at 4

°C for 10 min at 4000 ×g. The supernatant (170 µL) was transferred to a 500 µL 96-well plate and

dried under heated nitrogen (45°C). Samples were then reconstituted with 50 µL of water:methanol

(98:2) containing 0.1% formic acid, vortex-mixed for 1 min at 2000 rpm, followed by 10 min of

centrifugation at 4000g at 4 °C before MS analysis. To avoid PDA and HVA degradation, all

samples were protected from direct light exposure during sample preparation and analysis.

LC-MS/MS analyses were carried out on a Waters Acquity UPLC system, consisting of a

Acquity binary solvent manager and Acquity sample manager with sample organizer (Waters,

Milford, MA, USA) coupled to a SCIEX 6500 tandem quadrupole mass spectrometer (Applied

Biosystems/MDS SCIEX, Toronto, Canada) equipped with an ESI source. The analytes (10 µL)

were separated on an Acquity UPLC BEH130 C18 (2.1 x 100 mm; 1.7 µm particle size) column

and eluted by a gradient program as follows: held 2% B for 0.5 min, 2% B to 20% B in 2.5 min,

20% B to 98% B in 1 min, 98% B to 2% B in 0.01 min and retained 1 min for equilibration. The

column was heated at 45°C, and the flow rate was 500 µL/min. The mobile phase consisted of an

aqueous phase (A: 0.1% formic acid in water) and an organic phase (B: 0.1% formic acid in

acetonitrile).

The ESI source was operated in negative ion mode, and its main working parameters were

set as follows: ion spray voltage, -4.5 kV; ion source temperature, 550°C; declustering potential, -

40 V for PDA and HVA and -150 V for Enal-d5; collision energy, -35 V; entrance potential, -10

V; and collision cell exit potential, -10 V. Multiple reaction monitoring (MRM) measurements of

-4PA and HVA analytes were performed using individually optimized cone voltage and collision

energy. The MRM precursor/product ion transitions were as follows: m/z 182> 138.0 for PDA,

15

181.0 > 122.0 for HVA, and 380.3 > 114.2 for the internal standard, Enal-d5.The dwell time

established for each transition was 50ms. All peak integration and data processing were performed

using SCIEX Analyst 1.6.2 (Applied Biosystems/MDS SCIEX).

Pharmacokinetic, Transport and Statistical Analysis. The area under the plasma

concentration-time curve from zero to 24 h ($AUC_{0\text{-}24\ h}$) was calculated using mixed trapezoidal

rule. The area under the plasma concentration-time curve from zero to infinity (AUC) includes

$AUC_{0\text{-}24\ h}$ and one extrapolated to infinity from the last measured concentration. The volume of

distribution at steady-state (Vd_{SS}) was determined by noncompartmental method:

$$Vd_{SS} = \frac{Dose \bullet (AUMC)}{(AUC)^2}$$ Equation 1

where $AUMC$ is the area under the curve of the first moment of the concentration-time curve.

The total plasma clearance (CL_{TOT}) was calculated from:

$$CL_{TOT} = \frac{Dose}{AUC}$$ Equation 2

The pharmacokinetics parameters including $AUC_{0\text{-}24h}$, AUC, Vd_{SS}, and CL_{TOT} for FSM,

PROB, PDA and HVA, following single intravenous administration of PROB, FSM with or

without co-administration of PROB were analyzed with a mixed trapezoidal model using Kinetica

program (Thermo Electron; Philadelphia, PA). The renal clearance (CL_R) was estimated from:

$$CL_R = \frac{Xe_{0-24h}}{AUC_{0-24h}}$$ Equation 3

where $Xe_{0\text{-}24\ h}$ is the cumulative amount of unchanged FSM excreted in urine over 24 h. The renal

extraction ratio (ER_R) of FSM was calculated by the following equation:

$$ER_{\mathrm{R}} = \frac{CL_R}{f_u \bullet GFR}$$
<div align="right">Equation 4</div>

where f_{u} is the fraction of unbound FSM in human plasma reported (i.e., 0.041) (Rane et al., 1978), and *GFR* is the glomerular filtration rate in cynomolgus monkeys (i.e., 10.4 mL/min) (Davies and Morris, 1993). The fraction of FSM excreted unchanged in the urine (f_{R}) was calculated by dividing $Xe_{\text{0-24 h}}$ by the dose. Nonrenal plasma clearance(CL_{NR}) was estimated as the difference between the total plasma and renal clearances. The fraction excreted by nonrenal routes (f_{NR}) was calculated by dividing the nonrenal clearance by the total plasma clearance. Paired Student's *t*-test was performed to compare pharmacokinetic parameters between groups using GraphPad Prism version 7 (GraphPad Software, Inc., San Diego, CA). A *P*-value of less than 0.05 was considered to be statistically significant (* $P < 0.05$, ** $P < 0.01$, and *** $P < 0.001$). In order to compare pharmacokinetic parameter between groups, the data are also reported as geometric mean ratio with a two-sided 90% confidence interval (90% *CI*).

Transport data represent the results from a single study run in triplicate and a minimum of two experiments on different days. The results were reported as mean ± SD (n = 3). To estimate transport kinetics parameters of PDA and HVA into transporter-expressing HEK 293 cells, the transporter-mediated uptake was calculated by subtracting the uptake in MOCK-HEK cells from that in transporter-expressing HEK 293 cells. The following equation was used to estimate the parameters:

$$V = \frac{V_{\max} \mathrm{x}[S]}{K_{\mathrm{m}} + [S]}$$
<div align="right">Equation 5</div>

DMD # 77586

where V is the rate of uptake measured at the given concentration; $V_{\max}$ is the maximal rate of

uptake; K_{m} represents the Michaelis-Menten constant at which the transport rate is half its

maximal value and [S] is the substrate concentration.

Statistical differences between cell lines or treatments were determined by an unpaired

two-tailed Student t-test. (GraphPad Prism version 7; GraphPad Software, Inc.; San Diego, CA).

A P-value of less than 0.05 was considered to be statistically significant (* $P < 0.05$, ** $P < 0.01$,

and *** $P < 0.001$).

18

DMD # 77586

RESULTS

Effects of PROB on Pharmacokinetics of FSM in Cynomolgus Monkeys. Mean FSM plasma concentration-time profiles after IV administration of 2 mg/kg of FSM in the absence and presence of PROB (40 mg/kg, IV) are illustrated in Figure 2A. The plasma concentrations of FSM were higher in the presence than in the absence of PROB at all time points and in all animals. This statement was supported by the significant increase in $AUC_{0-24\,h}$ (11.5 ± 0.7 and 47.7 ± 5.0 μM•h after IV administration of 2 mg/kg FSM alone and with 40 mg/kg PROB, respectively; $P < 0.01$; Table 1). The geometric mean and 90% confidence interval (CI) of FSM $AUC_{0-24\,h}$ ratio were 4.1 (3.6 to 4.8). Consistently, the CL_{TOT} of FSM was reduced significantly by PROB pretreatment (8.8 ± 0.6 versus 2.1 ± 0.3 mL/min/kg; $P < 0.001$). However, the administration of PROB did not cause a significant difference in Vd_{SS} and terminal elimination half-life ($T_{1/2}$) of FSM although mean values were decreased by PROB pretreatment (0.33 ± 0.11 versus 0.21 ± 0.03 L/kg and 5.9 ± 1.4 versus 4.7 ± 0.8 h, respectively; $P > 0.05$) (Table 1).

Mean urinary excretion rates of FSM in cynomolgus monkeys are shown in Figure 2C. A 2.1- to 2.4-fold reduction of FSM urinary excretion in the presence of probenecid was observed ($P < 0.01$). The renal clearance (CL_R) and extraction ratio (ER) of FSM were reduced significantly with PROB pretreatment (3.7 ± 0.6 versus 0.44 ± 0.12 mL/min/kg and 49.5 ± 8.8 versus 5.9 ± 1.4, respectively; $P < 0.01$). Furthermore, the non-renal clearance of (CL_{NR}) of FSM in the presence of PROB was also reduced markedly (5.0 ± 0.6 versus 1.7 ± 0.2 mL/min/kg, respectively; $P < 0.01$). Therefore, the reduced CL_{TOT} by PROB pretreatment was not solely due to either decreased CL_R or CL_{NR}.

Figure 2B illustrates PROB concentration in plasma after IV PROB alone and concurrently with FSM. The PROB plasma concentrations at 24 h after PROB administration ($C_{24\,h}$) were not

19

significantly different (7.3 ± 5.7 and 8.9 ± 6.5 μM, $P > 0.05$). (Table 1). Comparing other PROB

pharmacokinetic parameters in the absence or presence of FSM indicates that the mean PROB

$AUC_{0-24\ h}$, $C_{24\ h}$, CL_{TOT} and $T_{1/2}$ values were almost identical (Table 1).

Identification of Potential Plasma Endogenous Biomarkers of OAT1 and OAT3 by

Metabolomics. To identify potential endogenous plasma probes of OAT1 and OAT3, LC-MS-

based metabolomics was used to determine the alterations in plasma concentrations of endogenous

compounds between treatments in cynomolgus monkeys. A total of 233 metabolites of known

structural identity by matching accurate mass and retention time values with in-house database of

endogenous metabolites were measured, and the concentration values used to determine statistical

significance using paired Student t-test (Supplementary Table 1). Of those metabolites monitored,

29 endogenous molecules were identified to be present at concentrations at least 3-fold higher at

1 h and/or 3 h in PROB pretreatment groups (administered alone or with FSM) (Table 2),

suggesting that the changes of endogenous metabolites in the plasma were associated with

inhibition of monkey OAT1 and OAT3, with associated reduction of OAT-mediated renal

clearance. However, only some metabolites were able to return to baseline at 24 h, which is

included as criterion for transporter biomarker candidate.

Based on the structure similarities, the identified metabolites can be categorized into three

subset groups. The first subset of metabolites are long-chain dicarboxylic acids and derivatives

(Table 2), which include tetradecanedioic acid (TDA) [$HOOC(CH_2)_{12}COOH$] and

hexadecanedioic acid (HDA) [$HOOC(CH_2)_{14}COOH$]. The second subset consists of small acids

that are produced by gut microflora. The metabolites include indole-3 acetic acid, cresol sulfate,

phenyl sulfate, phenyllactic acid, indoxyl sulfate, and phenylacetylglycine. The third are amino

acids and derivatives, which include hydroxy isovaleric acid, tyrosine, and aspartic acid. The

metabolites whose plasma concentrations were significantly increased by PROB pretreatments include PDA, HVA, glucuronic acid, pantothenic acid, xanthurenic acid, and kynurenic acid (Table 2). The administration of PROB caused increases in plasma PDA and HVA concentrations at 1 and 3 h (approximately 3- to 6-fold), and the concentrations returned to base line at 24 h (Table 2). PDA and HVA represent novel types of endogenous biomarkers not known previously to interact with monkey and human OAT1 and OAT3. Therefore, we conducted follow-up experiments to determine time-course of change in plasma PDA and HVA concentrations and transporter-expressing cell uptake that comprehend the sensitivity and specificity of the probes as described below.

Time-Dependent Effects on Plasma PDA, HVA, HDA and TDA Levels of PROB Pretreatment. Administration of 40 mg/kg PROB intravenously caused increases in plasma PDA and HVA concentrations in monkeys. The plasma PDA concentration increased by approximately 3-fold over the first 24 h (113.5 ± 23.3 and 120.0 ± 17.9 versus 40.5 ± 2.2 μM•h, $P < 0.05$), and gradually declined to the basal level (1.5 ± 0.3 μM) at 24 h after PROB pretreatment (Figure 3A and Table 3). The PDA concentrations were greater at any time points after PROB pretreatment compared to those after furosemide administration. Similarly, the increase in plasma HVA concentration was persistent. The plasma HVA concentration peaked at 3 to 4 h, returning to the base line (85 ± 32 nM) within 24 h after PROB pretreatment with approximately 2-fold increase in AUC (6.5 ± 1.0 and 8.7 ± 1.9 versus 4.1 ± 0.7 μM•h, $P < 0.05$) (Figure 3B and Table 3). As shown in Table 3, PROB pretreatment significantly decreased CL_R of PDA compared to FSM treatment ($P < 0.05$). The pretreatment also decreased CL_R of HVA although the reduction were not statistically significant.

We also detected the effects of PROB on plasma concentrations of TDA and HDA since they are reported as substrates of OAT1 and OAT3. PROB pretreatment increased plasma concentrations of TDA and other long chain dicarboxylic acids in monkeys (Table 2). Figures 3E and 3F show that PROB pretreatments increase plasma concentrations, although the increases were not statistically significant (Table 3).

Measurement of PDA and HVA Uptake in Stable Cell Lines Constitutively Expressing Renal Transporter. In order to determine whether PDA and HVA are substrates for major renal drug transporters, the cellular uptake of the molecules were measured at a single concentration (1 and 5 μM for PDA and HVA, respectively) in human OAT1-, OAT2-, OAT3-, OAT4-, OCT2-, MATE1-, MATE2K-, OATP1B1, OATP1B3-, and NTCP-HEK cells after a 5 min incubation. The cellular uptake of PDA and HVA into the HEK cells stably transfected with the cynomolgus monkey renal organic anion transporters was not evaluated because the in vitro models are not available in the United States (Tahara et al., 2005). The uptake of PDA in OAT1- and OAT3-HEK cells was approximately 55- and 52-fold higher than that in the control cells (1757 ± 703 vs. 30.6 ± 6.7 and 1548 ± 40.0 vs. 29.8 ± 5.9 pmol/mg/5 min, respectively) (Figure 4A). In addition, the PDA uptake in OAT1- and OAT3-HEK cells is significantly inhibited by PROB, a potent OAT1 and OAT3 inhibitor (Figure 4A). Furthermore, PDA is a substrate for human OAT4 because the uptake of PDA in OAT4-HEK cells is significantly greater than that in Mock-HEK cells (1.8-fold; $P < 0.01$) and the uptake is reduced by 1 mM PROB (Figure 5A). On the other hand, there was no significant OAT2-, OCT2-, MATE1-, and MATE2K-mediated uptake of PDA compared with the control ($P > 0.05$) (Figures 4A and 5A). Similarly, the uptake of HVA in OAT1 and OAT3-expressing cells was approximately 45- and 6-fold higher than those in the control cells (8.33 ± 0.40 vs. 0.18 ± 0.02 and 1.09 ± 0.09 vs. 0.18 ± 0.02 pmol/mg/5 min, respectively; $P <$

22

0.001) (Figure 4B). Additionally, there was also significant OAT2-mediated uptake of HVA compared with the control (5-fold; $P < 0.001$). However, there was no significant OCT2-, MATE1-, and MATE2K-mediated uptake of HVA compared with the control ($P > 0.05$). Moreover, both PDA and HVA are not substrates for human hepatic transporters OATP1B1, OATP1B3, and NTCP because there are no significant difference in the uptake between the transporter-overexpressing cells and mock cells ($P > 0.05$) (Supplemental Figure 2).

The affinities of OAT1- and OAT3 meditated transport for PDA and HVA were further determined over a range of PDA and HVA concentrations (0.2-500 µM) in OAT1- and OAT3-HEK cells after a 2.5-min incubation. The incubation time was set by the linear-uptake condition and the lower limit of bioanalytical methods (Supplemental Figure 1). As shown in Figure 6, the apparent K_{m} values were 33.0 ± 5.3 and 52.1 ± 15.3 µM for OAT1- and OAT3-mediated uptake of PDA, respectively, while the apparent K_{m} values of OAT1-, OAT-2 and OAT3-mediated uptake of HVA were 108 ± 6.2, 124 ± 10.8 and 438 ± 63 µM, respectively.

DISCUSSION

OAT transporters are mainly expressed in renal proximal tubular cells and mediate active renal secretion of their substrates. Inhibition of OAT transporter function could lead to decreased renal elimination and increased plasma exposure of xenobiotics and endogenous metabolites that are transported by these transporters. The general approach of using cynomolgus monkey as a model for study of human transporter function has become routine and takes advantage of the similarity and function of drug transporters between humans and monkeys (Shen et al., 2016b; Shen et al., 2013; Tahara et al., 2006). It is recognized that such approaches can identify endogenous biomarker candidates that are selective for specific transporter (Chu et al., 2015; Shen et al., 2016a; Thakare et al., 2017). To demonstrate that cynomolgus monkey permits quantitative prediction of human OAT-mediated DDIs, we measured the effects of the clinically relevant OAT inhibitor PROB on the pharmacokinetics of the OAT1 and OAT3 probe substrate FSM in monkeys, and compared these with the changes observed in human subjects. As shown in Figure 2, the intravenous administration of PROB generated a plasma total $C_{24\,h}$ of 7.3 ± 5.7 μM (Figure 2 and Table 1). Based on the IC_{50} values for both monkey OAT1 and OAT3 (< 10 μM) (Tahara et al., 2005), sustained inhibition of OAT1 and OAT3 transport function is anticipated. In agreement with the in vitro inhibition, a pronounced increase in AUC of FSM, a known substrate of OAT1 and OAT3, resulting from PROB pretreatment was evident (Figure 2 and Table 1). At the relevant dose (i.e., 40 mg/kg, IV), PROB decreased the FSM CL_R by 8.3-fold in cynomolgus monkeys. The decreases in the CL_R of coadministered FSM observed in the clinic were 3.6- to 5.1-fold for PROB (Chennavasin et al., 1979; Smith et al., 1980). Furthermore, PROB decreased FSM CL_{NR} in monkeys and humans by 2.9- and 1.5-fol, respectively, suggesting inhibition of FSM metabolism in both species. In the current study, we demonstrate that intravenous pretreatment of cynomolgus

24

monkeys with PROB (40 mg/kg) increased in the AUC of FSM by 4.1-fold consistent with the

values (3.1- to 3.7-fold) reported in humans, indicating that drug-drug interactions associated with

OAT transporter inhibitions could be reproduced in cynomoglous monkey. These results support

previous findings in cynomolgus monkeys where it was found that OAT1 and OAT3 exhibit very

similar transport kinetics compared to corresponding human orthologs, and cynomolgus monkeys

are recommended as more appropriate alternative systems for predicting DDIs involving renal

drug transporters in humans (Tahara et al., 2006; Tahara et al., 2005).

In the present study, we applied a combination of fit-for-purpose untargeted metabolomics

and quantitative multiple reaction monitoring LC-MS/MS methods (Figure 1) to determine if OAT

inhibition is associated with changes in plasma concentrations of endogenous metabolites that are

reflecting of OAT function. Of 233 plasma metabolites examined using metabolomics method, 29

metabolites including PDA and HVA were significantly increased at 1 or 3 h in plasma from

monkeys by PROB. Of those, a number of metabolites identified had not previously been reported

as substrates for OAT1 and OAT3 (Table 2). LC-MS/MS methods were further optimized for

determination of plasma PDA and HVA concentration-time profiles. We found that PDA and HVA

to be consistently elevated in plasma from cynomolgus monkeys pretreated with PROB alone and

with FSM ($AUC_{0-24 h}$ of 2.8- to 2.9-fold and 1.6- to 2.1-fold, respectively), similar to the increase

in plasma FSM concentration (4.1-fold) (Figures 2 and 3, and Tables 1 and 3). Furthermore, we

demonstrated that PDA and HVA are substrates for human OAT1, OAT3, OAT2 (HVA), and

OAT4 (PDA) but not OCT2, MATE1, MATE2K, OATP1B1, OATP1B3, and NTCP (Figures 4

and 5, and Supplemental Figure 2). However, we did not study the transport of PDA and HVA by

cynomolgus monkey OAT1 and OAT3 because the in vitro cell models are not available in the

United States. The species-dependent differences in OAT1- and OAT3-mediated transport of PDA

25

and HVA cannot be excluded although monkey OAT1 and OAT3 exhibit similar transport kinetics (i.e. K_m and V_{max} values) to human orthologs (Tahara et al., 2005). Collectively, the results from the present study demonstrate that circulating PDA and HVA can be potentially used as endogenous biomarkers of OAT1 and OAT3 inhibition.

A few years ago, an investigation was conducted examining the changes of plasma and urine metabolites with murine Oat1 (Slc22a6) deficiency. Using untargeted metabolomics analysis, the researchers identified several physiologically important metabolites, including PDA, that were increased in the plasma from Oat1 knockout mice compared with wild-type animals, suggesting they are substrates for mouse Oat1 (Wikoff et al., 2011). In agreement, PROB increased the plasma HVA levels in rhesus monkey (Bacopoulos et al., 1978). PDA has been shown to undergo active renal secretion in humans, and elevated plasma PDA was observed in patients with renal insufficiency (Coburn et al., 2002). It is worth noting that the present study shows a considerable variation in the urinary excretion and CL_R of PDA and HVA (Figures 3B and 3D and Table 3). In addition, the volumes of urine samples collected in PROB groups during normal diuresis and forced diuresis (i.e., administration of PROB alone and with FSM) are significantly different. Despite large variation, PROB pretreatments, either alone or with FSM, significantly reduced the CL_R values of PDA in monkeys (Ratios of 0.10 and 0.33-0.46, respectively), similar to the decrease in FSM CL_R [0.12 (0.11-0.13)] (Tables 1 and 3).

Although the plasma levels of HVA are significantly increased by PROB pretreatments compared with FSM treatment, the CL_R value was only slightly reduced by PROB pretreatments (Ratios of 0.8 and 0.49-0.50, respectively) and the changes were not statistically significant. It is unclear why PROB pretreatments decreased the CL_R of HVA to a lesser extent compared to PDA.

However, the following observations may shed some light. Based on the in vitro uptake experiments, the renal basolateral transporters OAT1, OAT2 and OAT3 are involved into the uptake of HVA while PDA is only transported by OAT1 and OAT3 (Figures 4 and 6). OAT2 is less sensitive to the inhibition by PROB compared to OAT1 and OAT3 (IC_{50} of 393 to 766 µM versus < 10 µM) (Enomoto et al., 2002; Jia et al., 2015). In contrast to our findings, previous studies examining expression of human organic anion transporters in the choroid plexus and their interactions with neurotransmitter metabolites have reported that HVA is not a substrate for human organic anion transporters OAT1 and OAT3 in mouse cells (second segment of the proximal tubule cells, S2 cells) stably expressing OAT1 or OAT3 (Alebouyeh et al., 2003). The difference in transport profiling is probably due to the use of different host cells (HEK 293 cells vs. S2 cells), and endogenous expression of mouse Oat1, oat2 and Oat3 in S2 host cells would mask HVA uptake. Although we showed high-affinity uptake of PDA and HVA by basolateral transporters OAT1, OAT3, and/or OAT2 into stably transfected HEK cells (Figures 4 and 6), the mechanism(s) of the export of PDA and HVA out of the proximal tubule cells into the urine is not fully understood. These molecules may be extruded out of the cell by efflux transporters multidrug resistance protein 2 and 4 (MRP2 and MRP4) since most MRP2 and MRP4 substrates are organic anions, which are localized in the apical membrane of renal proximal tubule cells. In addition, the renal apical transporter OAT4 may play a role in the transport of PDA from RPTCs into the urine since OAT4 can operate in efflux mode in addition to influx fashion (Hagos et al., 2007).

PROB is a selective inhibitor of OAT1 and OAT3 as its IC_{50} values towards other transporters are greater than 25 µM (Supplemental Table 2), although for other monkey transporters there is still paucity of complete data for PROB inhibition. Therefore, even though the results presented herein showcase PDA and HVA as novel cynomolgus monkey plasma OAT

biomarkers, it cannot be assumed that the results translate directly to human subjects. In addition, we cannot exclude that the formation of the biomarkers studied may be affected by PROB. Moreover, PDA is the dead-end catabolite of the B6 vitamins including pyridoxine, pyridoxamine, and pyridoxal (Merrill and Henderson, 1990). Although the plasma PDA baseline level exhibits acceptable inter-individual variability in monkeys and humans (1.6 ± 0.4 µM and 43 ± 17 nM) (Coburn et al., 2002), the use of vitamin B6 supplements causes elevation of PDA levels far above the normal physiological level (Coburn et al., 2002; Zempleni, 1995). Therefore, the use of vitamin B6 supplements should be excluded in a clinical study with the goal of assessing a change in PDA plasma level.

Emerging metabolomics and genome-wide association data revealed that HDA and TDA, two fatty acid dicarboxylates, were potential endogenous biomarkers of human OATP1B1 (Yee et al., 2016). Although HDA and TDA are substrates of OATP1B1, OAT1 and OAT3 were also involved the disposition of HDA and TDA (Yee et al., 2016). Consistently we have observed that administration of rifampin, a selective inhibitor of hepatic OATPs over renal OATs, increased the AUCs of HDA and TDA by approximately 2-fold in human subjects (Shen et al., 2017). Although these results indicated that HDA and TDA are endogenous biomarkers of OATP1B1, the in vitro transport profiling suggested the involvement of OAT1 and OAT3 in the disposition of HDA and TDA (Yee et al., 2016). Metabolomics analysis in this study demonstrated the significant elevations in plasma levels of at least 20 dicarboxylic acids and fatty acids in the monkeys pretreated with PROB (Table 2 and Supplemental Table 1). A similar trend was more evident for TDA with significant increases of *AUC* in the LC-MS/MS dataset (Figure 3C and Table 3). A comparable degree of increase has been observed with HDA (Figure 3D and Table 3). As a result, HDA and TDA may serve as dual hepatic OATP and renal OAT biomarkers although further

28

studies are needed for the relevance of clinical interactions. The concentration-time profiles for TDA and HDA appear different in the PROB alone and with FSM groups although the concentrations in both groups are greater than those in that of FSM alone (Figures 3C and 3D). This is likely due to the additional inhibitory effect of FSM toward OAT1- and OAT3-mediated transport of TDA and HDA (Hasannejad et al., 2004; Nieskens et al., 2016).

In conclusion, the use of monkey as a transporter-mediated DDI model along with metabolomics has been demonstrated to be a useful approach for transporter biomarker identification. Our investigations showed that PDA and HVA are novel blood biomarkers of monkey renal OAT as the changes in plasma exposures of PDA and HVA are similar to that of a probe substrate in monkeys. Although interspecies difference in the transport and disposition of PDA and HVA need be considered, information obtained in this monkey study on the extent of these endogenous compounds after pretreatment with PROB along with the results from stably transporter-overexpressing cell lines suggest that PDA and HVA are candidate biomarkers of OAT1 and OAT3 for use in clinical settings.

Acknowledgments

DMD # 77586

Authorship Contributions

Participated in research design: Shen, Nelson, Oliveira, Lai, and Humphreys.

Conducted experiments: Shen, Oliveira, Zhang, Mcnaney, Gu, Cheng, and Su.

Contributed new reagents or analytic tools: Shen, Nelson, and Oliveira.

Performed data analysis: Shen, Nelson, Oliveira, Zhang, Shipkova, Reily,

Gan, Marathe, and Humphreys.

Wrote or contributed to the writing of the manuscript: Shen, Nelson, Oliveira, Lai, Marathe, and

Humphreys.

.

References

Bergagnini-Kolev, M.C., Hebert, M.F., Easterling, T.R., and Lin, Y.S. (2017). Pregnancy Increases the Renal Secretion of N1-methylnicotinamide, an Endogenous Probe for Renal Cation Transporters, in Patients Prescribed Metformin. Drug metabolism and disposition: the biological fate of chemicals *45*, 325-329.

Chennavasin, P., Seiwell, R., Brater, D.C., and Liang, W.M. (1979). Pharmacodynamic analysis of the furosemide-probenecid interaction in man. Kidney international *16*, 187-195.

Chu, X., Chan, G.H., and Evers, R. (2017). Identification of Endogenous Biomarkers to Predict the Propensity of Drug Candidates to Cause Hepatic or Renal Transporter-Mediated Drug-Drug Interactions. Journal of pharmaceutical sciences *106*, 2357-2367.

Chu, X., Shih, S.J., Shaw, R., Hentze, H., Chan, G.H., Owens, K., Wang, S., Cai, X., Newton, D., Castro-Perez, J.*, et al.* (2015). Evaluation of cynomolgus monkeys for the identification of endogenous biomarkers for hepatic transporter inhibition and as a translatable model to predict pharmacokinetic interactions with statins in humans. Drug metabolism and disposition: the biological fate of chemicals *43*, 851-863.

Coburn, S.P., Reynolds, R.D., Mahuren, J.D., Schaltenbrand, W.E., Wang, Y., Ericson, K.L., Whyte, M.P., Zubovic, Y.M., Ziegler, P.J., Costill, D.L.*, et al.* (2002). Elevated plasma 4-pyridoxic acid in renal insufficiency. Am J Clin Nutr *75*, 57-64.

Davies, B., and Morris, T. (1993). Physiological parameters in laboratory animals and humans. Pharmaceutical research *10*, 1093-1095.

Enomoto, A., Takeda, M., Shimoda, M., Narikawa, S., Kobayashi, Y., Kobayashi, Y., Yamamoto, T., Sekine, T., Cha, S.H., Niwa, T.*, et al.* (2002). Interaction of human organic anion transporters 2 and 4 with organic anion transport inhibitors. J Pharmacol Exp Ther *301*, 797-802.

Hagos, Y., Stein, D., Ugele, B., Burckhardt, G., and Bahn, A. (2007). Human renal organic anion transporter 4 operates as an asymmetric urate transporter. Journal of the American Society of Nephrology : JASN *18*, 430-439.

Hasannejad, H., Takeda, M., Taki, K., Shin, H.J., Babu, E., Jutabha, P., Khamdang, S., Aleboyeh, M., Onozato, M.L., Tojo, A.*, et al.* (2004). Interactions of human organic anion transporters with diuretics. The Journal of pharmacology and experimental therapeutics *308*, 1021-1029.

Hnatyshyn, S., Shipkova, P., and Sanders, M. (2013). Expedient data mining for nontargeted high-resolution LC-MS profiles of biological samples. Bioanalysis *5*, 1195-1210.

Hsueh, C.H., Yoshida, K., Zhao, P., Meyer, T.W., Zhang, L., Huang, S.M., and Giacomini, K.M. (2016). Identification and Quantitative Assessment of Uremic Solutes as Inhibitors of Renal Organic Anion Transporters, OAT1 and OAT3. Mol Pharm *13*, 3130-3140.

Imamura, Y., Tsuruya, Y., Damme, K., Heer, D., Kumagai, Y., Maeda, K., Murayama, N., Okudaira, N., Kurihara, A., Izumi, T*., et al.* (2014). 6beta-Hydroxycortisol is an endogenous probe for evaluation of drug-drug interactions involving a multispecific renal organic anion transporter, OAT3/SLC22A8, in healthy subjects. Drug metabolism and disposition: the biological fate of chemicals *42*, 685-694.

Ito, S., Kusuhara, H., Kumagai, Y., Moriyama, Y., Inoue, K., Kondo, T., Nakayama, H., Horita, S., Tanabe, K., Yuasa, H*., et al.* (2012). N-methylnicotinamide is an endogenous probe for evaluation of drug-drug interactions involving multidrug and toxin extrusions (MATE1 and MATE2-K). Clinical pharmacology and therapeutics *92*, 635-641.

Jia, W., Du, F., Liu, X., Jiang, R., Xu, F., Yang, J., Li, L., Wang, F., Olaleye, O.E., Dong, J*., et al.* (2015). Renal tubular secretion of tanshinol: molecular mechanisms, impact on its systemic exposure, and propensity for dose-related nephrotoxicity and for renal herb-drug interactions. Drug metabolism and disposition: the biological fate of chemicals *43*, 669-678.

Lai, Y., Mandlekar, S., Shen, H., Holenarsipur, V.K., Langish, R., Rajanna, P., Murugesan, S., Gaud, N., Selvam, S., Date, O*., et al.* (2016). Coproporphyrins in Plasma and Urine Can Be Appropriate Clinical Biomarkers to Recapitulate Drug-Drug Interactions Mediated by Organic Anion Transporting Polypeptide Inhibition. The Journal of pharmacology and experimental therapeutics *358*, 397-404.

Mariappan, T.T., Shen, H., and Marathe, P. (2017). Endogenous Biomarkers to Assess Drug-Drug Interactions by Drug Transporters and Enzymes. Curr Drug Metab.

Merrill, A.H., Jr., and Henderson, J.M. (1990). Vitamin B6 metabolism by human liver. Ann N Y Acad Sci *585*, 110-117.

Mori, S., Takanaga, H., Ohtsuki, S., Deguchi, T., Kang, Y.S., Hosoya, K., and Terasaki, T. (2003). Rat organic anion transporter 3 (rOAT3) is responsible for brain-to-blood efflux of homovanillic acid at the abluminal membrane of brain capillary endothelial cells. J Cereb Blood Flow Metab *23*, 432-440.

Morrissey, K.M., Stocker, S.L., Wittwer, M.B., Xu, L., and Giacomini, K.M. (2013). Renal transporters in drug development. Annu Rev Pharmacol Toxicol *53*, 503-529.

Motohashi, H., Sakurai, Y., Saito, H., Masuda, S., Urakami, Y., Goto, M., Fukatsu, A., Ogawa, O., and Inui, K. (2002). Gene expression levels and immunolocalization of organic ion transporters in the human kidney. Journal of the American Society of Nephrology : JASN *13*, 866-874.

Muller, F., Pontones, C.A., Renner, B., Mieth, M., Hoier, E., Auge, D., Maas, R., Zolk, O., and Fromm, M.F. (2015). N(1)-methylnicotinamide as an endogenous probe for drug interactions by renal cation transporters: studies on the metformin-trimethoprim interaction. Eur J Clin Pharmacol *71*, 85-94.

Nieskens, T.T., Peters, J.G., Schreurs, M.J., Smits, N., Woestenenk, R., Jansen, K., van der Made, T.K., Roring, M., Hilgendorf, C., Wilmer, M.J.*, et al.* (2016). A Human Renal Proximal Tubule Cell Line with Stable Organic Anion Transporter 1 and 3 Expression Predictive for Antiviral-Induced Toxicity. AAPS J *18*, 465-475.

Nigam, S.K., Wu, W., Bush, K.T., Hoenig, M.P., Blantz, R.C., and Bhatnagar, V. (2015). Handling of Drugs, Metabolites, and Uremic Toxins by Kidney Proximal Tubule Drug Transporters. Clin J Am Soc Nephrol *10*, 2039-2049.

Peng, C.C., Templeton, I., Thummel, K.E., Davis, C., Kunze, K.L., and Isoherranen, N. (2011). Evaluation of 6beta-hydroxycortisol, 6beta-hydroxycortisone, and a combination of the two as endogenous probes for inhibition of CYP3A4 in vivo. Clinical pharmacology and therapeutics *89*, 888-895.

Rane, A., Villeneuve, J.P., Stone, W.J., Nies, A.S., Wilkinson, G.R., and Branch, R.A. (1978). Plasma binding and disposition of furosemide in the nephrotic syndrome and in uremia. Clinical pharmacology and therapeutics *24*, 199-207.

Rodrigues, A.D., Taskar, K.S., Kusuhara, H., and Sugiyama, Y. (2017). Endogenous Probes for Drug Transporters: Balancing Vision With Reality. Clinical pharmacology and therapeutics.

Shen, H., Chen, W., Drexler, D.M., Mandlekar, S., Holenarsipur, V.K., Shields, E.E., Langish, R., Sidik, K., Gan, J., Humphreys, W.G.*, et al.* (2017). Comparative Evaluation of Plasma Bile Acids, Dehydroepiandrosterone Sulfate, Hexadecanedioate and Tetradecanedioate with Coproporphyrins I and III as Markers of OATP Inhibition in Healthy Subjects. Drug metabolism and disposition: the biological fate of chemicals.

Shen, H., Dai, J., Liu, T., Cheng, Y., Chen, W., Freeden, C., Zhang, Y., Humphreys, W.G., Marathe, P., and Lai, Y. (2016a). Coproporphyrins I and III as Functional Markers of OATP1B Activity: In Vitro and In Vivo Evaluation in Preclinical Species. The Journal of pharmacology and experimental therapeutics *357*, 382-393.

Shen, H., Liu, T., Jiang, H., Titsch, C., Taylor, K., Kandoussi, H., Qiu, X., Chen, C., Sukrutharaj, S., Kuit, K.*, et al.* (2016b). Cynomolgus Monkey as a Clinically Relevant Model to Study Transport Involving Renal Organic Cation Transporters: In Vitro and In Vivo Evaluation. Drug metabolism and disposition: the biological fate of chemicals *44*, 238-249.

Shen, H., Yang, Z., Zhao, W., Zhang, Y., and Rodrigues, A.D. (2013). Assessment of vandetanib as an inhibitor of various human renal transporters: inhibition of multidrug and toxin extrusion as a possible mechanism leading to decreased cisplatin and creatinine clearance. Drug metabolism and disposition: the biological fate of chemicals *41*, 2095-2103.

Smith, D.E., Gee, W.L., Brater, D.C., Lin, E.T., and Benet, L.Z. (1980). Preliminary evaluation of furosemide-probenecid interaction in humans. Journal of pharmaceutical sciences *69*, 571-575.

Tahara, H., Kusuhara, H., Chida, M., Fuse, E., and Sugiyama, Y. (2006). Is the monkey an appropriate animal model to examine drug-drug interactions involving renal clearance? Effect of probenecid on the renal elimination of H2 receptor antagonists. The Journal of pharmacology and experimental therapeutics *316*, 1187-1194.

Tahara, H., Shono, M., Kusuhara, H., Kinoshita, H., Fuse, E., Takadate, A., Otagiri, M., and Sugiyama, Y. (2005). Molecular cloning and functional analyses of OAT1 and OAT3 from cynomolgus monkey kidney. Pharmaceutical research *22*, 647-660.

Thakare, R., Gao, H., Kosa, R.E., Bi, Y.A., Varma, M.V.S., Cerny, M.A., Sharma, R., Kuhn, M., Huang, B., Liu, Y.*, et al.* (2017). Leveraging of Rifampicin-Dosed Cynomolgus Monkeys to Identify Bile Acid 3-O-Sulfate Conjugates as Potential Novel Biomarkers for Organic Anion-Transporting Polypeptides. Drug metabolism and disposition: the biological fate of chemicals *45*, 721-733.

Tsuruya, Y., Kato, K., Sano, Y., Imamura, Y., Maeda, K., Kumagai, Y., Sugiyama, Y., and Kusuhara, H. (2016). Investigation of Endogenous Compounds Applicable to Drug-Drug Interaction Studies Involving the Renal Organic Anion Transporters, OAT1 and OAT3, in Humans. Drug metabolism and disposition: the biological fate of chemicals *44*, 1925-1933.

Vree, T.B., van den Biggelaar-Martea, M., and Verwey-van Wissen, C.P. (1995). Probenecid inhibits the renal clearance of frusemide and its acyl glucuronide. Br J Clin Pharmacol *39*, 692-695.

Wikoff, W.R., Nagle, M.A., Kouznetsova, V.L., Tsigelny, I.F., and Nigam, S.K. (2011). Untargeted metabolomics identifies enterobiome metabolites and putative uremic toxins as substrates of organic anion transporter 1 (Oat1). J Proteome Res *10*, 2842-2851.

Yee, S.W., Giacomini, M.M., Hsueh, C.H., Weitz, D., Liang, X., Goswami, S., Kinchen, J.M., Coelho, A., Zur, A.A., Mertsch, K*., et al.* (2016). Metabolomic and Genome-wide Association Studies Reveal Potential Endogenous Biomarkers for OATP1B1. Clinical pharmacology and therapeutics *100*, 524-536.

Zempleni, J. (1995). Pharmacokinetics of vitamin B6 supplements in humans. J Am Coll Nutr *14*, 579-586.

Footnotes

Reprint requests:

Dr. Hong Shen

Room F1.3802, Route 206 & Province Line Road, Princeton, NJ 08543

Bristol-Myers Squibb Company

Telephone: (609) 252-4509; Facsimile: (609) 252-6802

Figure Legends

Figure 1. Schematic overview of experimental workflow for identification and validation of endogenous biomarkers of OAT1 and OAT3. Plasma samples were collected from monkey FSM-PROB interaction study, and metabolites were quantified by LC coupled with MS. Raw data were extracted, and analyzed by various tools to identify associations between drug treatments and concentrations, determine significant correlations, and integrate results with transporter knowledge. Three selected potential endogenous biomarkers were further validated by LC-MS/MS with deuterated internal standards to confirm metabolomics observations. Transporter uptake studies were performed to determine whether the selected probes were selective substrates for human OAT1 and OAT3.

Figure 2. (A), Plasma concentration-time curves of FSM administered intravenously alone (2 mg/kg; open circles) or with PROB (40 mg/kg, IV; closed circles). (B), Plasma concentration time curves of PROB administered intravenously alone (40 mg/kg; open triangles) or with FSM (2 mg/kg, IV; closed triangles). (C), Effects of PROB on urinary exertion rate of FSM administered intravenously alone (2 mg/kg; open bar) or with PROB (40 mg/kg, IV; closed bar). Data are shown as mean ± SD (n = 3). **$P < 0.01$, significantly different from urinary excretion rate in the absence of PROB.

Figure 3. Effect of PROB on plasma concentration-time curves of PDA (A), HVA (B), TDA (C) and HDA (D) in 3 cynomolgus monkeys after intravenous administration of PROB alone (40 mg/kg; open squares), FSM alone (2 mg/kg, close triangles), and PROB with FSM (open circles).

38

Figure 4. Profiling of the transport of PDA and HVA by major drug transporters expressed at the basolateral membrane of RPTC. Uptake in the HEK cells stably transfected with the control vector (Mock-HEK), OAT1, OAT2, OAT3, or OCT2 was measured after a 5-min incubation at 37°C with PDA (1 μM) (A), HVA (5 μM) (B), and radio-labeled probe substrates [1 μM [^{3}H]PAH (OAT1), 1 μM [^{3}H]PCV (OAT2), 1 μM [^{3}H]E3S (OAT3), and 2 μM [^{14}C]MFM (OAT2)] (C). Incubations were conducted in the absence and presence of 1 mM PROB (OAT1 and OAT3), 100 μM IMC (OAT2), or 100 μM PYR (OCT2) to evaluate the effects of these inhibitors on PDA and HVA uptake. Each value represents the mean ± SD (n = 3). *P < 0.05, **P < 0.01 and ***P < 0.001 statistically significantly different from uptake in Mock-HEK cells, and $^\$P$ < 0.05, $^{\$\$}P$ < 0.01 and $^{\$\$\$}P$ < 0.001 statistically significantly different from uptake in the absence of an inhibitor.

Figure 5. Profiling of the transport of PDA and HVA by major drug transporters expressed at the apical membrane of RPTC. Uptake in the HEK cells stably transfected with the control vector (Mock-HEK), OAT4, MATE1, or MATE2K was measured after a 5-min incubation at 37°C with PDA (1 μM) (A), HVA (5 μM) (B), and [^{3}H]E3S (1 μM) and [^{14}C]MFM (2 μM) (C). Incubations were conducted in the absence and presence of 1 mM PROB (OAT4) or 100 μM PYR (MATE1 and MATE2K) to evaluate the effects of these inhibitors on PDA and HVA uptake. Each value represents the mean ± SD (n = 3). ***P < 0.001 statistically significantly different from uptake in Mock-HEK cells, and $^{\$\$\$}P$ < 0.001 statistically significantly different from uptake in the absence of an inhibitor.

Figure 6. Concentration-dependent uptake of PDA (A) and HVA (B) by human OAT1 and OAT3.

Cells were incubated with PDA or HVA (0.23 to 500 μM) for 2 min (linear range). The net OAT1-

(open triangle) or OAT3-mediated uptake (open circle) was calculated by subtracting that in mock

cells from that in OAT1- or OAT3-HEK cells. The curves represent the best fit of the Michaelis-

Menten equation. Each value represents the mean ± SD (n = 3).

Table 1. Pharmacokinetic Parameters of FSM and PROB in Cynomolgus Monkeys (n = 3) Following Intravenous Administration of PROB alone (40 mg/kg), FSM alone (2 mg/kg), and PROB with FSM

Analyte	Parameter	PROB alone	FSM alone	FSM with PROB	Ratio (90% CI)
FSM	$AUC_{0-24\ h}$ (µM•h)	NA	11.5 ± 0.7	47.7 ± 5.9**	4.1 (3.6-4.8)
	CL_{TOT} (mL/min/kg)	NA	8.8 ± 0.6	2.1 ± 0.3***	0.24 (0.21-0.28)
	Vd_{SS} (L/kg)	NA	0.33 ± 0.11	0.21 ± 0.03	0.66 (0.31-1.4)
	$T_{1/2}$ (h)	NA	5.9 ± 1.4	4.7 ± 0.8	0.82 (0.40-1.7)
	CL_R (mL/min/kg)	NA	3.7 ± 0.6	0.44 ± 0.12**	0.12 (0.11-0.13)
	CL_{NR} (mL/min/kg)	NA	5.0 ± 0.6	1.7 ± 0.2**	0.34 (0.27-0.42)
	ER_R	NA	49.5 ± 8.8	5.9 ± 1.4**	0.12 (0.11-0.13)
PROB	$AUC_{0-24\ h}$ (µM•h)	3,436 ± 655	NA	3,386 ± 860	0.98 (0.58-1.6)
	$C_{24\ h}$ (µM)	7.3 ± 5.7	NA	8.9 ± 6.5	1.1 (0.37-3.2)
	CL_{TOT} (mL/min/kg)	0.69 ± 0.12	NA	0.71 ± 0.18	1.0 (0.60-1.7)
	Vd_{SS} (L/kg)	0.20 ± 0.01	NA	0.21 ± 0.02	1.0 (0.85-1.3)
	$T_{1/2}$ (h)	3.7 ± 0.8	NA	3.7 ± 0.9	1.0 (0.87-1.1)

Pharmacokinetic parameters were determined as described in *Materials and Methods*. Data are shown as mean $\pm$ SD (n = 3). PROB was

intravenously dosed 30 min prior to FSM administration in the coadministration treatment group.

NA, not applicable. ** $p < 0.01$, and *** $p < 0.001$, when the parameter was compared with that administered with FSM or PROB alone.

Table 2. Comparison of Plasma Concentrations of the 29 Selected Endogenous Metabolites in Cynomolgus Monkeys (n = 3) Following Intravenous Administration of PROB alone (40 mg/kg), FSM alone (2 mg/kg), and PROB with FSM.

Metabolite Type	Metabolite Name	Ratio of PROB alone to FSM alone			Ratio of PROB with FSM to FSM alone		
		C_{1h}	C_{3h}	C_{24h}	C_{1h}	C_{3h}	C_{24h}
Dicarboxylic acids and derivatives	C18-di-OH dihydroxyoctadecanoic acid	5.1	7.6	2.1	11.7	9.5	2.5
	C18-2 dicarboxylic acid	3.2	3.7	0.8	8.6	5.1	0.8
	C20-4 dicarboxylic acid	3.0	3.6	0.7	8.8	5.5	0.5
	C18-1 dicarboxylic acid	2.7	3.6	0.7	7.8	5.8	0.5
	C16-1 dicarboxylic acid	2.4	2.0	0.6	4.6	2.8	0.8
	Tetradecanedioic acid (TDA)	2.3	3.7	2.6	8.8	13.7	2.0
	C12 dicarboxylic acid	2.1	3.7	1.2	1.8	2.4	2.0
	C10-1 dicarboxylic acid	2.1	2.8	0.7	3.4	4.5	0.7
	C12-1 dicarboxylic acid	2.1	1.2	0.9	3.1	1.7	0.8
	C12-OH hydroxydidecanoic acid	2.0	1.3	1.3	3.5	2.6	1.4
	C14-1 dicarboxylic acid	1.9	2.3	1.6	4.2	4.4	1.7
	Unsaturated tetradecanoyl carnitine (C14-1)	3.9	1.0	0.5	2.8	1.5	0.5
	Unsaturated lauryl carnitine (C12-1)	3.3	1.1	0.6	1.9	1.2	0.6
	Lauryl carnitine (C12)	3.0	1.1	0.5	1.7	0.9	0.5
Small acids produced by gut microflora	Indole-3 acetic acid	8.6	11.2	1.6	7.6	7.7	1.7
	Cresol sulfate	3.9	5.6	2.3	4.9	7.1	2.6

43

	Phenyl sulfate	3.1	2.9	1.5	2.6	3.4	1.6
	Phenyllactic acid	2.9	3.3	2.2	3.3	3.0	2.0
	Indoxyl sulfate	2.8	2.8	1.0	6.4	7.5	1.2
	Phenylacetylglycine	2.6	3.3	0.5	3.4	3.4	0.6
Amino acids and derivatives	Hydroxy-isovaleric acid	3.9	1.5	4.4	12.6	1.8	6.2
	Tyrosine	3.1	2.6	1.5	2.5	1.6	0.4
	Aspartic acid	2.2	3.0	2.2	1.6	2.5	0.5
Others	Pyridoxic acid (PDA)	4.5	4.8	1.4	5.6	6.0	1.5
	Homovanillic acid (HVA)	4.1	3.2	0.8	4.6	4.0	1.3
	Glucuronic acid	8.8	8.5	2.6	10.5	11.2	2.4
	Pantothenic acid	2.8	1.1	0.8	3.0	1.7	0.9
	Xanthurenic acid	3.8	5.2	0.4	7.4	8.1	0.7
	Kynurenic acid	3.5	4.1	0.6	6.6	6.0	1.0

Plasma concentrations of approximately 230 endogenous metabolites were determined by liquid chromatography-mass spectrometry (Supplementary Table 1). Each determination was made in samples collected at 1, 3, and 24 h post-dose from 3 cynomolgus monkeys, and values for compounds with ≥ 3.0-fold different plasma concentration at any of 3 time points in the monkeys treated with PROB and FSM are presented. P values were determined by paired Student's t test (Supplementary Table 1).

Table 3. Pharmacokinetic Parameters of PDA, HVA, HDA and TDA in 3 Cynomolgus Monkeys Following Intravenous Administration of PROB alone (40 mg/kg), FSM alone (2 mg/kg), and PROB with FSM.

Analyte	Parameter	PROB alone		FSM alone	FSM with PROB	
		Value	Ratio (90% CI)[a]	Value	Value	Ratio (90% CI)[a]
PDA	$AUC_{0-24\,h}$ (μM•h)	113.5 ± 23.3*	2.8 (2.0-3.9)	40.5 ± 2.2	120.0 ± 17.9**	2.9 (2.1-4.1)
	C_{max} (μM)	7.3 ± 1.2*	3.1 (2.2-4.3)	2.4 ± 0.2	7.9 ± 1.1**	3.3 (2.3-4.8)
	CL_R (mL/min/kg)	0.4 ± 0.2*	0.10 (0.01-1.6)	4.9 ± 3.3	2.7 (2.2 and 3.1)**[b]	0.39 (0.33 and 0.46)[b]
HVA	$AUC_{0-24\,h}$ (μM•h)	6.5 ± 1.0*	1.6 (1.1-2.3)	4.1 ± 0.7	8.7 ± 1.9*	2.1 (1.9-2.4)
	C_{max} (μM)	0.68 ± 0.03**	2.8 (2.0-3.8)	0.25 ± 0.04	0.78 ± 0.22*	3.1 (2.1-4.6)
	CL_R (mL/min/kg)	1.3 ± 0.5	0.8 (0.4-1.6)	1.6 ± 0.2	0.9 (0.9 and 0.8)*[b]	0.50 (0.49 and 0.51)[b]
TDA	$AUC_{0-7\,h}$ (nM•h)	449 ± 233*	2.8 (1.6-5.0)	168 ± 121	526 ± 250	3.3 (1.1-10.3)
	C_{max} (nM)	97 ± 43*	2.3 (1.8-3.0)	42 ± 21	195 ± 110	4.3 (1.1-17.7)
HDA	$AUC_{0-7\,h}$ (nM•h)	592 ± 224*	1.9 (0.9-3.7)	355 ± 263	870 ± 321	2.7 (0.9-8.0)
	C_{max} (nM)	148 ± 109	2.0 (1.1-3.9)	69 ± 45	223 ± 107*	3.3 (1.7-6.6)

Pharmacokinetic parameters were determined as described in *Materials and Methods*. Data are shown as mean ± SD (n = 3). PROB was

intravenously dosed 30 min prior to FSM administration in the coadministration treatment group.

[a] Ratio of pharmacokinetics parameter of PROB treatment to FSM treatment.

[b] Cage malfunction prevented urine collection from one monkey in the coadministration treatment group (n = 2).

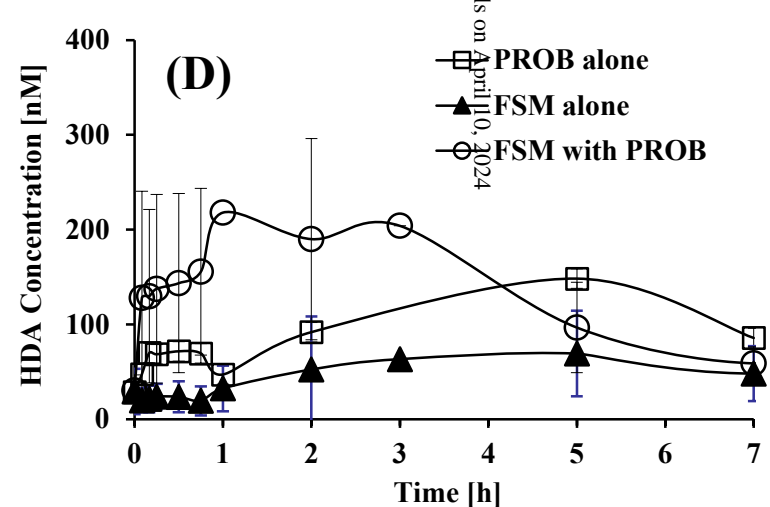* $P < 0.05$ and ** $P < 0.01$, when the parameter was compared with that administered with FSM alone.

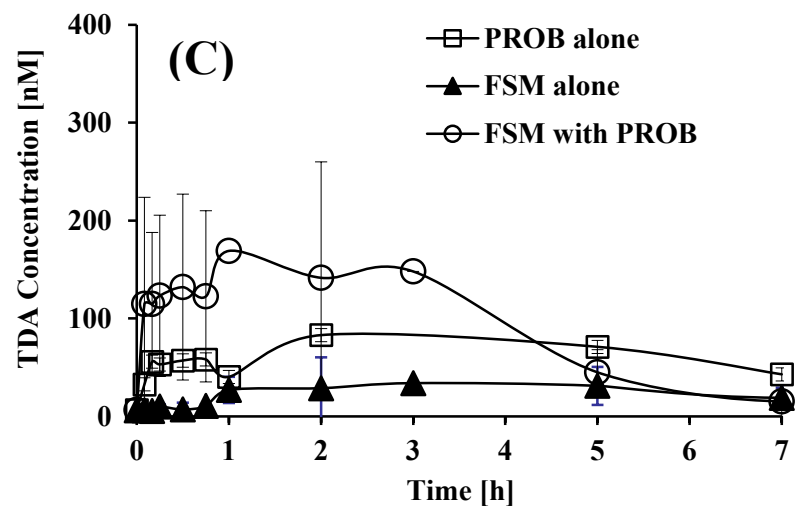**Plasma Sample Collection from Monkey DDI Study**

Metabolomics Data Acquisition

Data Alignment and Analysis Considering Experimental Factors

Period I
PROB alone

Period II
FSM alone

Period III
FSM-PROB

- **Time-Course of Changes in Plasma Levels of PDA, HVA, HDA and TDA Validation**

- **PDA and HVA Transport in OAT1- and OAT3-HEK Cells Validation**

PotentialOAT1/3 Endogenous Biomarkers Identification

Figure 1

Figure 2

Figure 3

A). PDA Uptake by Basolateral Transporters

B). HVA Uptake by Basolateral Transporters

C). Probe Uptake by Basolateral Transporters

Figure 4

A). PDA Uptake by Apical Transporters

B). HVA Uptake by Apical Transporters

C). Probe Uptake by Apical Transporters

Figure 5

Figure 6